Bulletin of the Disaster Prevention Research Institute Vol. 14, Part 2, February, 1965

80. Fundamental Study on Mud-flow

By Katsumasa YANO and Atsuyuki DAIDO

(Manuscript received October 20, 1964)

Abstract

The present paper deals with the deformation and flow of muddy clay or heavy sediment-concentration liquid. A fundamental procedure for solving the problem in this paper rests on the principle of the rheological consideration. A theoretical examination was carried out for the deformation of muddy clay with time and the flow of muddy clay and relatively small sediment-concentration liquid in open channels. Also experiments were conducted in order to verify the above theoretical treatment and to make clear the characteristics of muddy clay. The experiments showed that the theoretical treatment is valid for explaining the behavior of muddy clay and the flow of relatively small sediment- concentration liquid.

1. Introduction

As a first step in investigating mud-flow, the present paper deals with the deformation and flow of muddy clay or heavy sediment-concentration liquid. Mud-flow means the flow of the terrestrial deposit layer saturated with rain in a mountain stream. In Japan, many human lives and possessions are lost by the mud-flow every year. In addition, because of the occurrence of mud-flow, the river bed rises and mud-flow breaks structures in a river.

In order to prevent these disasters, the character of mud-flow should be made clear. Although there are many ways of approach in investigating mud-flow, the problem is treated here especially from the view point of establishing the mechanics of the flow.

First, this paper deals with the rheological law of muddy clay. The problems of the creep of muddy clay and the deformation law of such soil are discussed in Chapter 2.

In Chapter 3, we discuss the flow of muddy clay in an open channel in which the clay is loaded by the stress, τ greater than the yield stress τ_y.

In Chapter 4, the rheological property of the lower layer with heavy sediment-concentration near the bed in the flow of liquid with relatively small concentration is discussed.

2. Deformation and flow of muddy clay

Generally, material such as muddy clay deforms following the rheological law. The Bingham law or the pseudoplastic law applies to mud-flow. The Bingham plastic is characterized by the flow curve of a straight line having the yield stress τ_y expressed by an intersection with the shear-stress axis as shown in Fig. 1. The yield stress τ_y is the stress to exceed before the flow occurs. The rheological equation for the Bingham plastic may be written

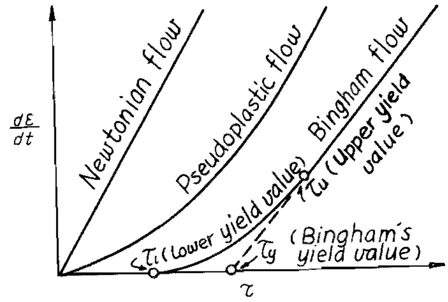

Fig. 1. Explanation diagram of flow curves.

$$\dot{\gamma}=\frac{\tau-\tau_y}{\mu_B} \qquad (1)$$

where $\dot{\gamma}$ is the rate of strain $d\epsilon/dt$ and μ_B the plastic viscosity.

The pseudoplastic flow has not any value of the yield stress and the typical flow curve for such materials indicates that the ratio of shear stress to the rate of strain, which may be termed the apparent viscosity μ_a is not constant, but decreases with increase in the rate of strain and that the flow curve becomes approximately linear only at very high rates of strain as shown in Fig. 1. The logarithmic plot of the rate of strain against the shear stress in this case is often found to be linear. As a result, the following empirical expression is widely used to characterize a fluid of this type:

$$\dot{\gamma}=\frac{\tau^n}{\mu_p} \qquad (2)$$

where μ_p is the pseudoplastic viscosity and n a constant expressing the degree of non-Newtonian behaviour.

However, it is not clear which materials this relation will fit and what characters these parameters have.

It is obvious that at least two parameters must be made for any non-Newtonian fluid by measurements in order to determine its rheological properties. To do this, the properties of muddy clay have been investigated by using a coaxial cylinder viscometer.

The relation between the measured torque T and the angular velocity ω of the inner cylinder for the Bingham plastic filled in the coaxial cylinder viscometer, is given by[1]

$$\omega=\frac{T}{4\pi h\mu_B}\left(\frac{1}{r_1^2}-\frac{1}{r_2^2}\right)-\frac{\tau_y}{\mu_B}\ln\frac{r_2}{r_1} \qquad (3)$$

where h is the depth of liquid and r_1 and r_2 are radii of the inner and outer cylinders respectively. Hence if ω is plotted against $\frac{T}{4\pi h}\left(\frac{1}{r_1^2}-\frac{1}{r_2^2}\right)$, the relation will be expressed by a straight line with a slope of $1/\mu_B$ when T exceeds the yield value of torque $2\pi\tau_y r_2^2 h$.

Therefore, by measuring the angular velocity and torque in the coaxial cylinder viscometer and plotting the relation between ω and $\frac{T}{4\pi h}\left(\frac{1}{r_1^2}-\frac{1}{r_2^2}\right)$, the values of μ_B and τ_y, can be decided.

On the other hand, for the pseudoplastic, the relation between T and ω is given by

$$\omega=\frac{1}{2n\mu_p}\left(\frac{T}{2\pi h}\right)^n\left(\frac{1}{r_1^{2n}}-\frac{1}{r_2^{2n}}\right) \qquad (4)$$

Hence if log ω is plotted against log T, the relation will be expressed by a straight line with a slope n. Some results of the tests conducted by these authors are shown in Fig. 2. From these graphs, it can be judged that the material is plastic. Eq. 1 explains the parts which are straight lines in Fig. 2. The details will be described in the following chapter.

It is seen, however, in Fig. 2 that the slow flow appears even when $\tau<\tau_y$. Such slow flow is as important as in the region of a high rate of strain for the mud-flow.

Some of the results of the tests for creep by shear are given in Fig. 3 showing curves of angular velocity ω under constant stresses in which the time t is taken as an abscissa.

The deformation of materials at a given moment of time t, is the sum of the recoverable and unrecoverable parts of deformations. The former is proportional to the stress; that is an elastic part. The latter is related to the rate of strain; that is a viscous part.

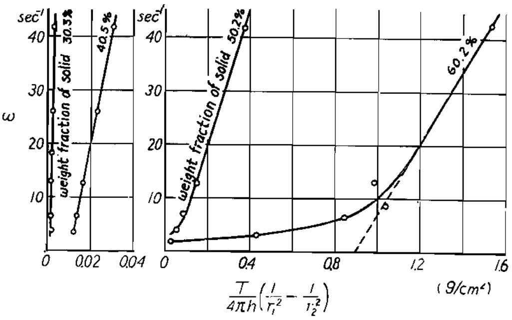

Fig. 2. Relations between ω and $\frac{T}{4\pi h}\left(\frac{1}{r_1^2}-\frac{1}{r_2^2}\right)$ for Bingham body.

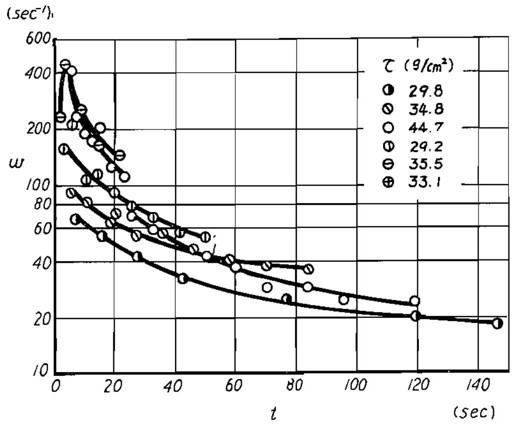

Fig. 3. Relations between angular velocity ω and time t.

The behavior of an ordinary viscoelastic body is characterized by a modulus of elasticity γ and a coefficient of viscosity μ, and the shear stress is expressed by

$$\tau=\gamma\cdot\epsilon+\mu\frac{d\epsilon}{dt} \tag{5}$$

The solution of Eq. 5 is

$$\epsilon=e^{-\frac{\gamma}{\mu}t}\left(\epsilon_0+\frac{1}{\mu}\int_0^t\tau\cdot e^{\frac{\gamma}{\mu}t}dt\right) \tag{6}$$

where ϵ_0 is the strain at $t=0$. When $\tau=$constant, Eq. 6 becomes

$$\epsilon=\frac{\tau}{\gamma}+\left(\epsilon_0-\frac{\tau}{\gamma}\right)e^{-\frac{\gamma}{\mu}t} \tag{7}$$

if ϵ_0 is zero, Eq. 7 is written as

$$\epsilon=\frac{\tau}{\gamma}\left(1-e^{-\frac{\gamma}{\mu}t}\right) \tag{8}$$

Therefore, the strain rate is

$$\frac{d\epsilon}{dt}=\frac{\tau}{\mu}e^{-\frac{\gamma}{\mu}t} \tag{9}$$

Since $d\epsilon/dt=\omega$, the following equation is introduced:

$$\log\omega=\log\frac{\tau}{\mu}-\frac{\gamma}{\mu}t\log e \tag{10}$$

Eq. 10 means a linear relation between $\log\omega$ and t.

It is fond, however, from the plots of data that this relation is generally not linear but concave as shown in Fig. 3 and the values of ω tend to be constant with the lapse of time. The difference in the tendency is caused by the assumption made in deriving Eq. 10 that γ and μ are constant. This phenomenon is always seen in the creep of a viscoelastic materials.

Therefore, the following equation will be used instead of Eq. 5:

$$\tau=\gamma(\epsilon)+\mu(\epsilon)\frac{d\epsilon}{dt} \tag{11}$$

The behavior of materials for which the stress-strain relationship is expressed by Eq. 11 may be described by the integral equation of Boltzmann[2]. The deformation at a certain time t, caused by a stress varying with time is expressed as follows:

$$\epsilon(t)=\frac{\tau(t)}{\gamma}+\int_0^t g(t-\xi)\tau(\xi)d\xi \tag{12}$$

At a constant stress, the equation takes the form

$$\epsilon(t)=\frac{\tau}{\gamma}+\tau\int_0^t g(t-\xi)d\xi \tag{13}$$

When the stress τ workes from $\xi(<t)$ to $\xi+d\xi$, the deformation during that time is the sum of the deformations ϵ_1 and $-\epsilon_2$, in which ϵ_1 is the deformation from ξ to t in Eq. 13 and $-\epsilon_2$ is the deformation from $\xi+d\xi$ to t.

$$\epsilon_1(t)-\epsilon_2(t)=\tau\int_0^{t-\xi}g(t-\xi)d\xi-\tau\int_0^{t-\xi-d\xi}g(t-\xi-d\xi)d\xi \tag{14}$$

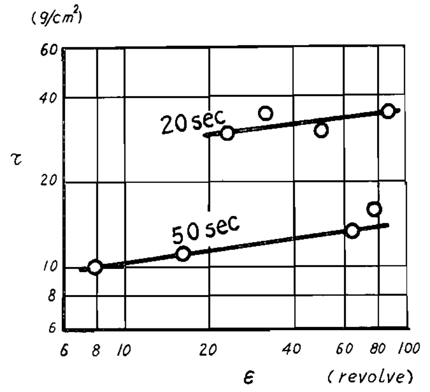

Fig. 4. Relations between stress τ and deformation ϵ with a parameter of time.

The deformation at time t is the sum of the instantaneous deformation and the deformation progressing with time. The latter is the integral of Eq. 14 from $t=0$ to $t=t$.

Since it is difficult to solve Eq. 14, the expression for the deformation after a certain time is written in the following form from experimental results shown in Fig. 4:

$$\epsilon=\lambda\tau^{\varphi} \tag{15}$$

where λ is a function of t and φ is a constant. Then, Eq. 15 is used instead of the first term of the right hand in

Eq. 14, in the same way as that of Nakano's treatment[4].

Similarly the second term is expressed in the following form:

$$\lambda\tau^{\varphi}+\frac{d\lambda}{dT}\tau^{\varphi}dT \tag{16}$$

where $T=t-z$. Thus

$$\epsilon_1(t)-\epsilon_2(t)=-\frac{d\lambda(T)}{dT}\tau^{\varphi}dT \tag{17}$$

Integrating Eq. 17 from $t=0$ to $t=t$ and adding the instantaneous deformation at time t, the following expression is derived for the total deformation at time t:

$$\epsilon(t)=\frac{\tau}{\gamma}-\tau^{\varphi}\int_t^0\frac{d\lambda(T)}{dT}dT=\frac{\tau}{\gamma}+\tau^{\varphi}\int_0^t\frac{d\lambda(T)}{dT}dT \tag{18}$$

Putting

$$\frac{d\lambda(T)}{dT}=\kappa(t) \tag{19}$$

then, Eq. 18 is written as

$$\epsilon(t)=\frac{\tau}{\gamma}+\tau^{\varphi}\int_0^t\kappa(t)dt \tag{20}$$

From the plots of data shown in Fig. 5, the ratio of the deformation to that at the upper limit of the yield point may be expressed as follows:

$$\epsilon/\epsilon_u=(t/t_u)^b \tag{21}$$

where ϵ_u is the value of deformation at the upper limit of the yield point, and t_u is a duration time until the deformation reaches the value ϵ_u.

Next, using Eq. 21 as the expression for the deformation at any time, from Eq. 20 the following relation is obtained:

$$\tau^{\varphi}\int_0^t\kappa(t)dt=\epsilon_u\left(\frac{t}{t_u}\right)^b \tag{22}$$

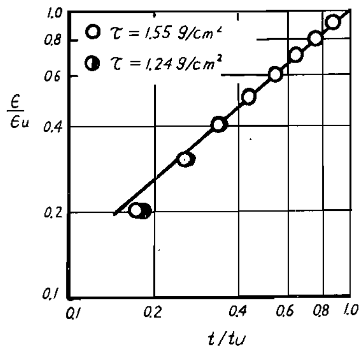

Fig. 5. Relation between ϵ/ϵ_u and t/t_u.

or

$$\kappa(t)=\frac{\epsilon_u}{\tau^{\varphi}}b\left(\frac{t}{t_u}\right)^b\frac{1}{t} \tag{23}$$

in which the value of b can be regarded constant, independent of the stress τ from the experimental results. For instance, when the concentration by weight c_g is 45.5 per cent, the value of b is 0.96.

The deformation to be added after it exceeds the upper limit of the yield point is expressed as

$$\epsilon=\frac{1}{\mu_B}(\tau-\tau_y)(t-t_u) \tag{24}$$

Therefore, the deformation at time t ($<t_u$) is written as

$$\epsilon(t)=\frac{\tau}{\gamma}+\tau^{\varphi}\int_0^{t_y}\kappa(t)dt+\frac{1}{\mu_B}(\tau-\tau_y)(t-t_u) \tag{25}$$

This equation is available for use when muddy clay is loaded by a stress τ which is greater than τ_y.

3. Flow of muddy clay in open channels

When τ is greater than τ_y, the muddy clay flows. The character of the flow in open channels is discussed in this chapter.

a) Bingham flow

The following equations are derived in general for uniform flow in an open channel.

$$(1-z/h)=\tau/\tau_0 \tag{26}$$

$$\tau_0=\rho g h I_e \tag{27}$$

where z is the distance from the bed, h the depth of flow, τ_0 the shear stress at the bottom, ρ the density of the fluid, and I_e the energy slope. Substituting Eq. 26 and 27 into Eq. 1, the expression for the velocity distribution is obtained as follows:

$$u=\frac{h\tau_y}{\mu_B}\left\{\frac{\zeta\left(a'-\frac{\zeta}{2}\right)}{1-a'}\right\} \tag{28}$$

where a' is equal to z_y/h, z_y the depth at the point were τ_y appears, and $\zeta=z/h$. In this case, the velocity reaches maximum value at $z=z_y$. Substituting $\zeta=a'$ into Eq. 28 yields

$$u_{max}=\frac{h\tau_y}{\mu_B}\left\{\frac{a'^2}{2(1-a')}\right\} \tag{29}$$

The mean velocity is

$$u_m=\frac{\int_0^{z_y} u dz+u_{max}(h-z_y)}{h}=\frac{h\tau_y}{\mu_B}\beta, \qquad \beta=\frac{a'^2\left(1-\frac{a}{3}\right)}{2(1-a')} \tag{30}$$

Then, the relation between the slope I and the mean velocity u_m is expressed as follows:

$$I=\frac{\tau_0}{\rho g h}=\frac{3u_m\left\{\frac{\mu_B}{3\beta(1-a')}\right\}}{\rho g h^2} \tag{31}$$

Now, putting

$$\mu_a=\frac{\mu_B}{3(1-a')\beta}$$

Eq. (31) corresponds to the resistance law for the laminar flow of the Newtonian liquid. Also, the resistance coefficient f' is introduced by the following expression:

$$I=f'\frac{1}{R}\frac{u_m^2}{2g} \tag{32}$$

For Bingham liquid, even when the mean velocity is the same, the velocity gradient on a boundary, or the boundary shear stress, is varied with the variation of τ_y or μ_B. Therefore, the resistance coefficient f' does not always correspond uniquely to the mean velocity u_m[5].

Then, the specified velocity U which is expressed as

$$U^2=\frac{1}{z_y}\int_0^{z_y}u^2dz=u_m^2F_{B1}(a), \qquad F_{B1}(a)=\frac{24}{5}\frac{1}{9-6a'+a'^2} \tag{33}$$

is adopted here instead of u_m.

In this case, the velocity U is different from u_m in Eq. 32. The velocity distribution for the laminar Newtonian flow is given by

$$u=\frac{\tau_0}{\mu_B}\left(z-\frac{z^2}{2h}\right) \tag{34}$$

then,

$$U^2=\frac{1}{h}\int_0^h u^2dz=\frac{1}{7.5}\left(\frac{\tau_0}{\mu_B}h\right)^2 \tag{35}$$

The mean velocity for laminar Newtonian flow in an open channel is

$$u_m^2=\frac{1}{9}\left(\frac{\tau_0}{\mu_B}\right)^2h^2 \tag{36}$$

Therefore, the value of F_{B1} in Eq. 33 becomes 1.2 for laminar Newtonian flow.

Thus, the energy slope for the Newtonian flow is expressed as

$$I=f'_N{}^*\frac{1}{h}\frac{U^2}{2g}=1.2f'_N{}^*\frac{1}{h}\frac{u_m^2}{2g}=f'_N\frac{1}{h}\frac{u_m^2}{2g} \tag{37}$$

where $f'_N=1.2f'_N{}^*$ and the suffix N denotes the resistance coefficient for the Newtonian flow. The expressions for the Bingham flow are

$$I=f'_B{}^*\frac{1}{h}\frac{U^2}{2g}=F_{B1}(a)f'_B{}^*\frac{1}{h}\frac{u_m^2}{2g} \tag{38}$$

or

$$f'_B=\frac{1.2\cdot 2ghI}{u_m^2F_{B1}(a)} \tag{39}$$

where the suffix B denotes the quantities for the Bingham flow.

In order that the relation between the resistance coefficient f'_{B1} and the Reynolds Number R_{eB} for the laminar Bingham flow may hold the expression $f'_B=6/R_{eB}$ for the Newtonian liquid, the Reynolds Number R_{eB} should be written as

$$R'_{eB}=\frac{\dfrac{\rho u_m h F_{B1}(a)}{1.2\mu_B}}{3\beta(1-a')} \tag{40}$$

b) *Pseudoplastic flow*

In the same way as to the Bingham liquid, Eqs. 26 and 27 are also applied to the uniform pseudoplastic flow. Substituting Eqs. 26 and 27 into Eq. 2 the expression for the vlocity distribution is obtained follows:

$$u=\frac{h\tau_0{}^n}{(n+1)\mu_p}\{1-(1-\zeta)^{n+1}\} \tag{41}$$

Therefore, the mean velocity is expressed as

$$u_m=\frac{1}{h}\int_0^h u dz=\frac{h\tau_0}{(n+2)\mu_p} \tag{42}$$

and the energy slope is

$$I=\frac{\tau_0}{\rho gh}=\frac{\mu_p^{1/n}u_m^{1/n}(n+2)^{1/n}}{\rho gh^{1+1/n}} \tag{43}$$

when $n=1$, Eq. 43 coincides with Eq. 38 for the laminar Newtonian flow.

In this case, even when the mean velocity is the same, the velocity gradient is varied with the value of n. In the same way as for the Bingham liquid, the following equations are derived:

$$U^2=\frac{1}{h}\int_0^h u^2 dz=u_m^2F_{p1}(n)$$

$$F_{p1}(n)=\frac{(n+2)^2}{(n+1)^2}\left\{1-\frac{2}{n+2}+\frac{1}{2(n+1)+1}\right\} \tag{43}$$

$$f'_p{}^*=\frac{1.2\cdot 2ghI}{u_m^2F_{p1}(n)} \tag{44}$$

$$R'_{ep}=\frac{3}{(n+2)^{1/n}u_m^{1/n}}\frac{\rho h^{1/n}u_m^2F_{p1}(n)}{1.2\mu_p^{1/n}} \tag{45}$$

where the suffix p denotes the quantities for the pseudoplastic flow.

c) Comparison between the experiment and the theory

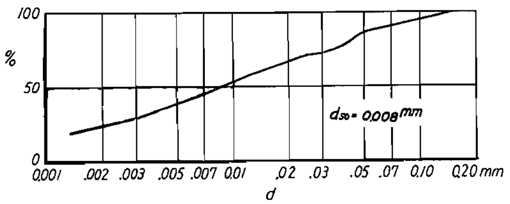

Fig. 6. Cumulative diagram of grain size distribution of sediment used.

TABLE 1.
Ranges of experiment.

conditions of flow	ranges
discharge	5— 20 l/sec
depth	5— 14 cm
concentration	0—350 gr/l
bed slope	1/100

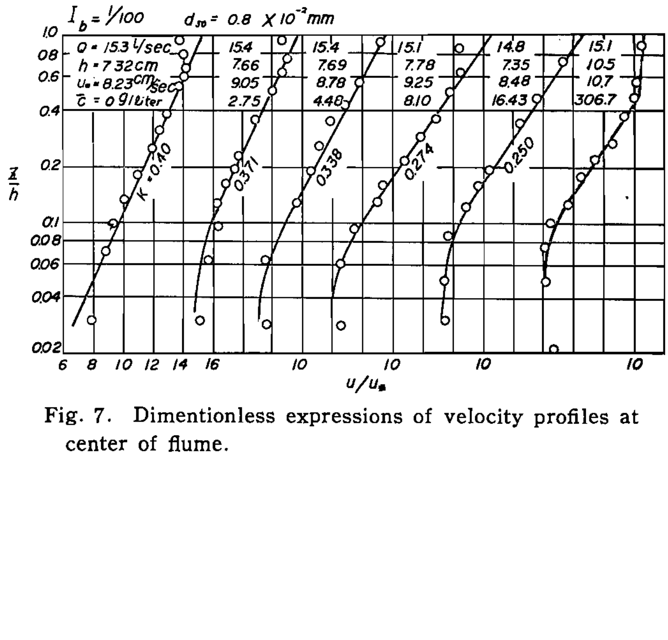

Fig. 7. Dimentionless expressions of velocity profiles at center of flume.

For the purpose of verifying the theoretical treatment described above and also of disclosing the characters of the mud-flow, experiments were carried out by using a steel channel of 0.2 m width and 20 m length and the clay of 0.8×10^{-2} mm in mean dimeter as shown in Fig. 6 under the condition shown in Table 1. Velocity distributions were observed by the applied Pitot tube method[6]. Some examples of the experimental results for velocity distribution are shown in Fig. 7.

Since it is found from the results of the experiments that in the case of the concentration $c_g>300$ g/l the velocity above a certain depth being almost constant, the flow in such a case was treated as that of Bingham liquid.

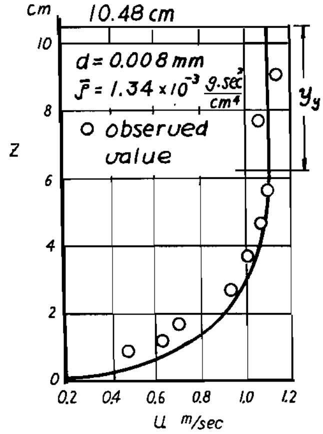

Fig. 8. Comparison of velocity profiles obtained by experiment and theory.

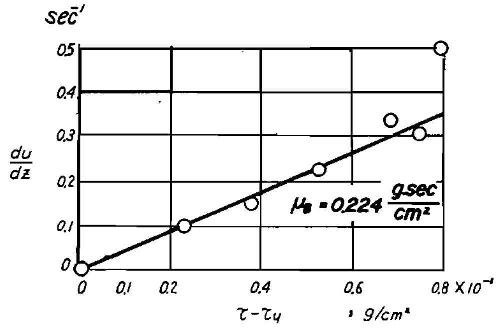

Fig. 9. Relation between du/dz and $\tau-\tau_y$ for data shown in Fig. 8.

A typical example of the velocity distributions under this condition is shown in Fig. 8. It seems that τ_y occured at $z=6.25$ cm, and therefore the relation between $(\tau-\tau_y)$ and du/dz is plotted as shown in Fig. 9. From this result, the material is considered as a Binghum fluid. The viscosity is not always constant over the flow layer. The viscosity near the upper limit of the yield point is estimated as 0.224 g·sec/cm². The velocity distribution calculated by using the above value is shown in Fig. 8. As there is very little data, the validity of Eqs. 39 and 40 were not checked for open channels, but the data of pipe flow was checked.

In pipe flow, the following equations are introduced corresponding to Eqs. 39 and 40 by the procedure similar to that for the Bingham liqued in an open channel :[6]

$$f_B=\frac{h_f}{l}\frac{D\cdot 2g}{u_m F_{B2}(a)}, \qquad F_{B2}(a)=\frac{9(5+6a-11a^2)}{5(3+2a+a^2)}\doteqdot 1-a \tag{45}$$

$$R_{eB}=\frac{4a\beta_2\rho D u_m^2 F_{B2}(a)}{\mu_B}, \qquad a=\frac{\tau_y}{\tau_0}, \qquad \beta_2=\frac{a^4-4a+3}{12a} \tag{46}$$

On the other hand, for the pseudoplastic liquid, the resistance coefficient and the Reynolds number are

$$f_p=\frac{h_f}{l}\frac{D\cdot 2g}{u_m^2 F_{p2}(n)} \qquad F_{p2}(n)=\frac{3}{4}\frac{n+3}{n+2} \tag{47}$$

$$R_{ep}=\frac{6(n+3)^{1-1/n}}{2}\frac{\rho u_m^{2-2/n}}{\mu^{1/n}} \tag{48}$$

where D is diameter of pipe, h_f the loss of head.

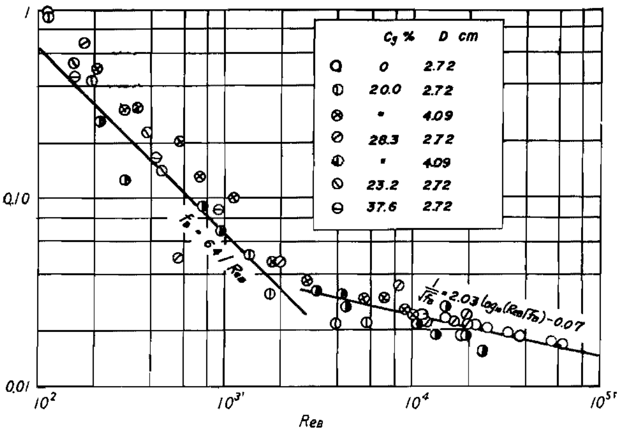

Fig. 10. Relation between f_B* and R_{eB} for Bingham flow in pipes.

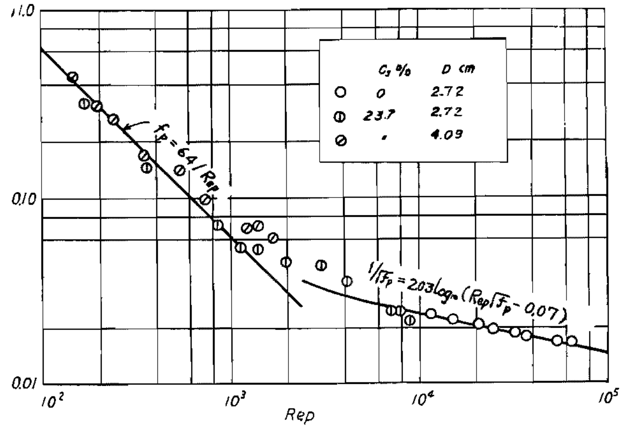

Fig. 11. Relation between f_p* and R_{ep} for pseudoplastic flow in pipes.

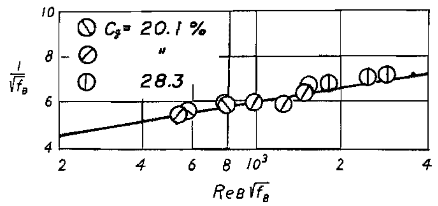

Fig. 12. Relation between $1/\sqrt{f_B}$ and $R_{eB}\sqrt{f_B}$ for Binghamflow in pipes.

Results of the experiment which was conducted by using plastic pipes of 2.72 cm and 4.09 cm in diameter for the Bingham and Newtonian flows are shown in Fig. 10. It is seen from this figure that the above relations may be adopted not only for apparent laminar flow but also for apparent turbulent flow. The word "apparent" is used here corresponding to the relation between the resistance coefficient and the Reynolds number for the Newtonian flow.

Fig. 11 shows the data for the pseudoplastic and Newtonian flows. It is considered that this expression is also applicable to apparent turbulent flow. It is found from Fig. 12 in which the relation between $1/\sqrt{f_B}$ and $R_{eB}\sqrt{f_B}$ is plotted that the resistance law of non-Newtonian flow is expressed as

$$\frac{1}{\sqrt{f_B}} = A + B\log_{10}(R_{eB}\sqrt{f_B}) \qquad (49)$$

where A and B are constant. For instance, in the case of Fig. 12, $A = -0.07$ and $B = 2.0$. The resistance law in pipe flow obtained by the authors for clear water is

$$\frac{1}{\sqrt{f}} = 2.0\log_{10}(R_e\sqrt{f}) - 0.07, \qquad (50)$$

Therefore, if the resistance law of non-Newtonian flow is expressed by the modified Reynolds number defined by Eq. 46 or 48, the values of A and B in Eq. 49 are equal to those for the Newtonian flow. However, it is generally known that $A=-0.8$ and $B=2.03$ for the Newtonian flow. Accordingly, the resistance law of the non-Newtonian flow for Bingham liquid in a pipe may be expressed as

$$\frac{1}{\sqrt{f_B}}=2.03\log_{10}(R_{eB}\sqrt{f_B})-0.8 \tag{51}$$

For the pseudoplastic, R_{eB} and f_B in Eq. 51 can be replaced by R_{ep} and f_p respectively. In an open channel, referring to the experimental result for the Newtonian flow in open smooth channels by Iwagaki[7], the relation described above, will be written as

$$\frac{1}{\sqrt{f'_B}}=2.07+4.07\log_{10}(R'_{eB}\sqrt{f'_B}) \tag{52}$$

4. Characteristics of flow with low sediment concentration

The data of the flow with low concentration in the previous experiments are treated in this chapter as the Newtonian flow by applying the logarithmic law of velocity distribution expressed by

$$\frac{u}{u_*}=A+\frac{1}{K}\ln\frac{z}{k_s} \tag{53}$$

where, u_* is the friction velocity, K the universal constant, A a constant and k_s the equivalent roughness.

In the flow with suspended materials, there are two problems for the velocity gradient. One is the increase of the velocity gradient in the upper region of flow, i.e. the decrease of the universal constant, and the other is the problem that the lograithmic law does not apply near the bed

Vanoni[8] and Ismail[9] pointed out the former problem based on experimental study. A theoretical explanation of this problem, was studied by Einstein and Chien[10], Tsubaki[11], Shimura[12] and Hino[13].

Einstein and Chien[10], and Ishihara, Iwagaki and Sueishi[6] pointed out the latter problem by their experimental data. But the mechanism was not mentioned sufficiently. According to the experiment by the authors, the thickness of the region is reached to 15 per cent of the water depth.

The phenomenon in this region seems to be very complicated because of being near the boundary, and in addition, it is very difficult to measure the velocity distribution. Therefore, as a first step, the flow in the region is treated as non-Newtonian flow.

For the upper region, Eq. 53 is used. Taking αk_s as the thickness of the lower region, and u_0 as the velocity at $z=\alpha k_s$, the distributions of velocity and sediment concentration are expressed respectively as follows.

$$\frac{u}{u_*}=\frac{u_0}{u_*}+\frac{1}{K}\ln\frac{z}{\alpha k_s} \tag{54}$$

$$\frac{C}{C_{\alpha ks}}=\left\{\frac{h-z}{z}\frac{\alpha k_s}{h-\alpha k_s}\right\}^{\frac{w_s}{Ku_*}} \tag{55}$$

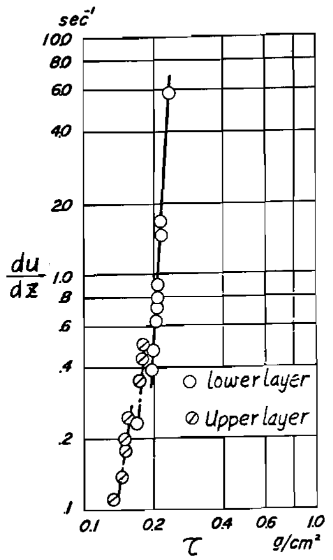

Fig. 13. Relation between du/dz and τ in lower layer of sediment laden flow.

where $C\alpha k_s$ is the concentration at $z=\alpha k_s$ and w_s the settling velocity.

The flow in the lower region is treated as the pseudoplastic, because it is generally known that a flow with a concentration of over 3 per cent is of pseudoplastic liquid and that of over 5 per cent is of a Bingham liquid. The validity of this treatment was checked by the data of Einstein and Chien[10]. From their data, it was found obviously that the logarithmic law cannot be applied to the lower region. The relation between $\log\tau$ and $\log du/dz$ in the lower layer is shown as a streight line in Fig. 13.

Using the expression of the velocity distribution for the lower layer, u_p is written as follows.

$$u_p=\frac{h\tau_0^n}{(n+1)\mu_p}\{1-(1-\zeta)^{n+1}\} \tag{56}$$

Then, the velocity u_0 at $z=\alpha k_s$ is

$$u_0=\frac{h\tau_0^n}{(n+1)\mu_p}\left\{1-\left(1-\frac{\alpha k_s}{h}\right)^{n+1}\right\} \tag{57}$$

Therefore, the mean velocity u_m is expressed as

$$\begin{aligned} u_m&=\frac{1}{h}\left\{\int_0^{\alpha k_s}u_p dz+\int_{\alpha k_s}^h u\cdot dz\right\}\\ &=(1-\eta)\frac{\tau_0^n h}{(n+1)\mu_p}\left\{1-\frac{1}{n+2}\frac{1-\eta^{n+2}}{1-\eta}\right\}+\eta\left\{\frac{u_0}{u_*}+\frac{1}{K}\ln\frac{h-\alpha k_s}{\alpha k_s}-\frac{1}{K}\right\}\\ &=(1-\eta)u_{mp}+\eta\cdot u_{mn} \end{aligned} \tag{58}$$

where

$$u_{mp}=\frac{\tau_0^n h}{(n+1)\mu_p}\left\{1-\frac{1}{n+2}\frac{1-\eta^{n+2}}{1-\eta}\right\} \tag{59}$$

$$u_{mn}=\frac{u_0}{u_*}+\frac{1}{K}\ln\frac{h-\alpha k_s}{\alpha k_s}-\frac{1}{K} \tag{60}$$

$$\eta=1-\frac{\alpha k_s}{h} \tag{61}$$

As a result, the mean velocity of the flow with law concentration is expressed in the form of the sum of the Newtonian and non-Newtonian regions.

If the low region is thin and therefore negligible, the above equation becomes the well-known equation by taking $\eta=1$ as follows:

$$\frac{u_m}{u_*}=A-\frac{1}{K}+\frac{1}{K}\ln\frac{h}{k_s} \tag{62}$$

where A is shown as [10]

$$A=\frac{10^{K/0.132}}{35.45} \tag{63}$$

a) *Universal constant K*

The universal constant K decreases with increase in the concentration. The theoretical explanation of this effect has been given by some researchers as previously mentioned. Fig. 14 shows the plots of experimental results according to the explanation of Shimura[12], which fits in fairly well with the theory. In the figure, a is the height of roughness, g the acceleration of gravity, γ_s the specific gravity of sediment particles, and c the volume concentration.

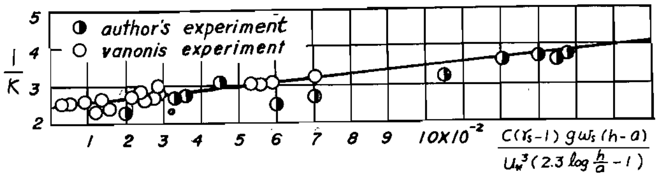

Fig. 14. Relation between $1/K$ and $\frac{c(\gamma_s-1)gw_s(h-a)}{u_*^3\left(2.3\log\frac{h}{a}-1\right)}$

b) *Thickness of lower layer*

Since αk_s is the thickness of the lower layer to which the mixing length theory can be applied, the Richardson number Θ, showing the stability of flow with density gradient[15], is adopted as a criterion to decide the value of αk_s, because when $\Theta>1$, the theory of momentum transport can be used. Richardson number Θ is given by the following expression:

$$\Theta\equiv\left(\frac{du}{dz}\right)^2\Big/-\frac{g}{\bar{\rho}}\frac{d\rho}{dz} \tag{64}$$

Letting ρ_0 and ρ_s be the densities of liquid and sediment particles respectively, the density of the liquid with sediment is expressed by

$$\rho=(\rho_s-\rho_0)c+\rho_0 \tag{65}$$

The basic equation of sediment suspension is given by

$$\varepsilon_s\frac{dc}{dz}+w_sc=0 \tag{66}$$

where ε_s is the sediment transfer coefficient. By Eqs. 65 and 66, the density gradient is written as.

$$\frac{d\rho}{dz}=-\frac{w_sc(\rho_s-\rho)}{\varepsilon_s} \tag{67}$$

Since the velocity gradient is

$$du/dz=u_*/Kz \tag{68}$$

The condition that Θ is greater than 1, is expressed as

$$\left(\frac{u_*}{Kz}\right)^2>\frac{gw_sc(\rho_s-\rho_0)}{\bar{\rho}\varepsilon_s} \tag{69}$$

Furthermore, ε_s in Eq. 69 is

$$\varepsilon_s=u_*Kz\left(1-\frac{z}{h}\right) \tag{70}$$

Thus,

$$\frac{\left(\frac{u_*}{Kz}\right)^2 u_* Kz\left(1-\frac{z}{h}\right)}{gw_s(\rho_s-\rho_0)} > c \tag{71}$$

Letting c_c be the concentration when Θ is equal to 1, and assuming αk_s is equal to the height from the bed when $c = c_c$, equation (71) becomes

$$\left(\frac{\rho_s-\rho_0}{\bar{\rho}}\right)c_c = \frac{u_* I}{Kw_s}\left(\frac{h}{\alpha k}-1\right) \tag{72}$$

In order to check the validity of Eq. 72 derived under the assumption that $z = k_s$ where the Richardson number is equal to one, experimental data obtained by Einstein and Chien[10] is used here. Fig. 15 represents the comparison between the value of αk_s obtained from Eq. 72 by using the measured value of K that evaluated from the experimental data of velocity distribution. In this case, the value of αk_s evaluated from the data is taken as the values of distance from the bed at which the velocity profile starts to deviate from a straight line in the semi-logarithmic plot in the table of the data by Einstein and Chien. In Fig. 15, the data when the value of $\alpha k_s/h$ is less than 0.05 have been omitted because the exact value of concentration at $z = \alpha k_s$ is not found in the table for that case. As shown in the figure, when the value of c_c is taken as that at $z = \alpha k_s$, the value of αk_s obtained from Eq. 72 is less than the value evaluated from the data. Therefore, is seems from Fig. 15 that the value of c_c is better taken as a mean value over the lower layer.

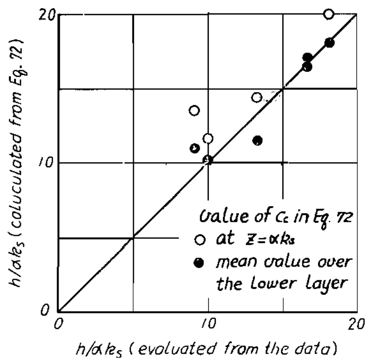

Fig. 15. Comparison of αk_s obtained by experiment and theory.

5. Summary and Conclusion

In this paper, the deformation and the flow of muddy clay or heavily concentrated liquid with sediment were treated from a rheological point of view. In Chapter 1, it was mentioned that the study of mud flow is very important in Japan.

In Chapter 2, it was shown that the deformation is expressed by Eq. 25, based on Boltzmann's idea and that the equation is suitable when the deformation is below the upper limit of the yield point.

In Chapter 3, the flow of muddy clay in open channels was treated. The relation between the resistance coefficient f and the Reynolds number for non-Newtonian flow was discussed and it was found that the modified Reynolds number proposed here is very useful for the "apparent" turbulent region.

In Chapter 4, the layer near the bed in the flow with relatively small sediment concentration was discussed. Since the velocity in this layer deviates from the logarithmic law of velocity distribution applied to the region of mainflow, the cross section of flow was divided into two parts the upper and the lower, which were treated as Newtonian flow and pseudoplastic flow respectively. It was found that the thickness of the lower layer can be evaluated on the basis of the condition that the Richardson number is equal to one at the boundary between the upper and lower layers.

Reference

1) Nakagawa, T. and Kanbe, T. : Rheology, Mimizu Shobo, 1950, p. 324 (in Japanese).
2) Nakagawa, T. and Kanbe, T. : Ref. 1) p. 372.
3) Vialov, S. S. and Skibitsky, A. M. : Rheolgical Processes in Frozen Soils and Dense Clays, Proc. 4th. International Conference on Soil Mechanics and Foundation Engineers, 1957, p. 125.
4) Nakano, Y. : Study on Rheolgical Character of Soil on Land Slide, Abstract of Papers the Annual Meeting of the A.E.C.J., 1961, p. 12 (in Japanese).
5) Tomita, Y. · Practical Treatment of Non-Newtonian Flow, Journal of the J.S.M.E., Vol. 63, 1959, p. 1596 (in Japanese).
6) Ishihara, T., Iwagaki, Y. and Sueishi, T. On the Velocity Measurement of Water Flow with Sediment Transportation. Bulletin of the Engineering Research Institute, Kyoto University, Vol. 5, 1954, p. 31 (in Japanese).
7) Iwagaki, Y. : On the laws of Resistance to Turbulent Flow in Open Smooth Channels, Proc. of the 2nd Japan National Congress for App. Mech. 1952, May 1953, pp. 245-250.
8) Vanoni, A. . Transportation of Suspended Sediment by Water, Proc. A.S.C.E., June. 1944, pp. 793-823.
9) Ismail, M. . Turbulent Transfer Mechanism and Suspended Sediment in Closed Channels, Trans, A.S.C.E., Vol. 117, 1952, pp. 499-446.
10) Einstein, H. A. and Chien, N. : Effect of Heavy Sediment Concentration near the Bed Velocity and Sediment Distribution, Corps. of Engineer Sediment Study Program for Missouri River Basin.
11) Tsubaki, T. : On the Effects Suspended Sediment on the Flow Characteristics, J.S.C.E., Vol. 40, 9, 1953, p. 1 (in Japanese).
12) Shimura, Y. : On the Characters of the Water Flow Containing Suspended Sediment, Trans. of the J.S.C.E., Vol. 46, 1957, p. 154 (in Japanese).
13) Hino, M. · The Changes in Turbulent Structure of Flow with Suspended Solid particles. Trans. of the J.S.C.E. No. 92, April, 1953, p. 11 (in Japanese).
14) Einstein, H. A. and Chien, N. : Ref. 9), p. 29.
15) Goldstein, S. : Modern Developments in Fluid Dynamics, Oxford University Press, 1952, p. 229.